

Specialized Spring Design in Segmented Edgewise Orthodontics: Further Verification of Dedicated Software

Domenico Mazza, MD, DDS^a; Michele Mazza, Mech Eng^a

Abstract: A software program for use in the investigation of specialized springs used in the segmented arch technique has previously been developed and an example of its clinical application has been shown. The purpose of this study was to further assess the reliability of the software in 4 tests using T-loop springs. A numerical simulation of a determined experimental condition relative to a T-loop spring was carried out in each test. Numerical and experimental results were compared, and the precision of the analytical tool was assessed relative to a variety of parameters of the spring. Since the comparison between numerical and experimental results showed good agreement along the entire range of activation of the spring, the reliability of the software is sufficient for the clinical purposes of the segmented arch technique. (*Angle Orthod* 2000;70:52–62.)

Key Words: Spring design, Dedicated software, Experimental-analytical comparison

INTRODUCTION

In the segmented arch technique, either specialized springs in their preactivation shapes or continuous ideal arches (or segments of an ideal arch) are used.¹ The specialized springs are used to move the teeth and are engaged in the attachments only at their ends. These springs are first bent into their passive shape in relation to the attachments, and then permanently deformed by incorporating suitable bends (preactivation bends) to apply the required force system to the tooth or teeth to be moved.

This new shape is called the *preactivation* or *deactivation shape*. When the preactivated spring is engaged into the attachments, it converts into the activation shape.

The usual experimental or analytical methods used in engineering can be applied to the study of the following problems relative to the specialized springs: (1) identification of the optimal spring for a required dental movement, and (2) determination of the preactivation shape of the optimal spring.

Experimental approach

In clinical use of the segmented arch technique, the preactivation shape of simpler springs, such as the intrusive arch² or tip-back springs,³ can easily be determined in the

dental clinic through a trial-and-error method coupled with use of a dynamometer. For the other specialized springs, the preactivation shape is first precalibrated in the laboratory using a spring tester measuring apparatus,⁴ which determines the uniplanar forces and moments. This preactivation shape is then photographed at a 1:1 magnification and presented as a template for clinical use.¹ This system is valid only in cases where templates have been provided. Special tables have recently been provided to obtain more templates.⁵

The optimal type of spring for retraction of anterior teeth is the T-loop spring.⁶ Three basic TMA (Titanium Molybdenum Alloy) T-loop spring designs⁸ have been developed for use in space closure, depending on the clinical geometry:

1. A composite anterior retraction spring, consisting of an 0.018" T-loop positioned mesially along the interbracket distance (IBD) and welded to a 0.017" × 0.025" base arch (Figure 1A, solid line).
2. A 0.017" × 0.025" posterior protraction spring with the T placed distally along the IBD (Figure 2A, solid line).
3. A 0.017" × 0.025" attraction spring with the T centered along the IBD (only the preactivation shape of this spring is shown in Figure 3A, solid line).

The mesial or α end of the T-loop spring is vertically offset 1 mm occlusally; the distal end is called β .

When pulled horizontally, the moments released from the 3 aforementioned basic TMA T-loop springs were insufficient to obtain the required dental movement, as shown by clinical experience. For this reason, the springs have been permanently deformed by the placement of preactivation

^a Private practice, Rimini, Italy.

Corresponding author: Domenico Mazza, MD, DDS, Studio di Clinica Odontoiatrica, Via Tempio Malatestiano, 12, 47900 Rimini (RN) Italy, (e-mail: dmazza@iper.net).

Accepted: June 1999. Submitted: January 1999.

© 2000 by the Edward H. Angle Society of Orthodontists

bends. These preactivation shapes have been precalibrated for a specific IBD using the spring tester.

An experimental study was then conducted in which the 3 basic TMA T-loop springs were examined relative to 4 different IBDs of clinical significance.⁸

The spring to be tested is mounted in parallel chucks, one of which is vertically offset 1 mm. One chuck is free to slide along a horizontal axis through a movable carriage. Transducers are connected with the chucks in order to measure either the force systems acting on them or the displacement of the moveable carriage (Appendix 1). Specifically, the alpha (anterior) and beta (posterior) moments and the horizontal and vertical forces were measured.

Analytical approach

The first analytical approach to solve problems relative to orthodontic springs was to idealize them as an assembly of straight beams and then analyze each using the small deflection beam theory (a linear theory).⁹

Using this approach, it was impossible to calculate the correct preactivation shape of the orthodontic springs, because the behavior of orthodontic springs is nonlinear, especially due to the great deflections commonly used with these springs. Such was the status until development of the finite element method and nonlinear analysis which, coupled with the rapid growth of modern computers, allowed a quantum jump forward in the computation of the behavior of these springs.

Four series of analytical studies investigating specialized orthodontic springs have been made. In each of these studies, some specific software was used to simulate analytical, numerical, and experimental conditions and compare the results. The percentage of approximation has been reported for some of these comparisons.

In the first series of studies, both linear and nonlinear finite element methods were used to investigate the large deformation behavior of nonpreactivated appliances.^{10,11} Experimental data were also obtained to confirm the analytical model. Results of the nonlinear solutions agreed with the experimental results.

In the second series of studies, an analytical nonlinear finite difference method was developed for determining the forces and moments in the 3 planes of space that are developed by any complex orthodontic appliance undergoing large activations.^{12,13} Both linear and nonlinear solutions were calculated for a number of appliances, including a stainless steel, symmetrical, T-loop spring (not preactivated) with a nominal rectangular cross section $0.01'' \times 0.02''$ pulled horizontally 2 mm.¹⁴ The experimental results were within 10% of the numerical value. Furthermore, a suitable algorithm was proposed to determine the preactivation shape of the transpalatal arch.¹⁵

In the third series of studies, the above stainless steel, symmetrical, nonpreactivated T-loop spring was investigat-

ed experimentally and numerically.¹⁶ The numerical simulation was done using a generic powerful finite-element commercial package, using either a linear or a nonlinear approach. Again, the approximation between experimental and numerical results was within 10%. Differences between linear and nonlinear solutions were also small, thus emphasizing that deflections and rotations for this case were relatively small.¹⁷ It has been critically concluded that the approach used in the second series of studies was capable of handling nonlinear solutions only when the deformations were small.

The same nonlinear commercial package was used to numerically simulate a symmetrical, preactivated TMA T-loop spring with a $0.017'' \times 0.025''$ rectangular cross section.¹⁶ This spring was subjected to neutral activation and then to horizontal activation. Agreement between the nonlinear solution and experiment was within 15%, which was arbitrarily recognized as sufficient from a practical viewpoint. However, extensive computational time was necessary. The linear solution for the same spring yielded results largely different from the experimental ones due to the relatively large rotations. For this reason, this case was estimated to be able to act as a suitable test to verify the nonlinear capability of the software.

None of the asymmetric cases of the spring were evaluated with the same package due to the excessive computational time required.¹⁶ The use of a nonlinear commercial package is not recommended for computing the behavior of orthodontic springs because of the cost and skill required and because the computational time is too long.

Another numerical procedure known as the segmental technique has been recommended and used to investigate the large deformations of orthodontic appliances.^{17,18} This procedure has been expanded to consider the complete 3-dimensional aspects of wire deformation.¹⁹ The segmental technique was used to compute the previously used symmetric, nonpreactivated stainless steel T-loop spring, with results that were similar to the nonlinear results obtained using the commercial package.¹⁷ A preactivated and slightly asymmetric TMA $0.017'' \times 0.025''$ T-loop spring was also simulated using the segmental technique.¹⁷ The spring was subjected to neutral activation and then to horizontal activation. The agreement between nonlinear simulation and the experiment was within 10%.

Unlike the commercial package, the computations using the segmental technique can be performed on a personal computer in a reasonable amount of time. Furthermore, some possible factors of difference between experimental and theoretical results have been emphasized as small differences between actual and analytical geometries, and as small differences in the moduli of elasticity between different authors.

In this series of studies, the preactivation shapes of the T-loop springs that were numerically simulated were previously determined experimentally.^{16,17} But once the prob-

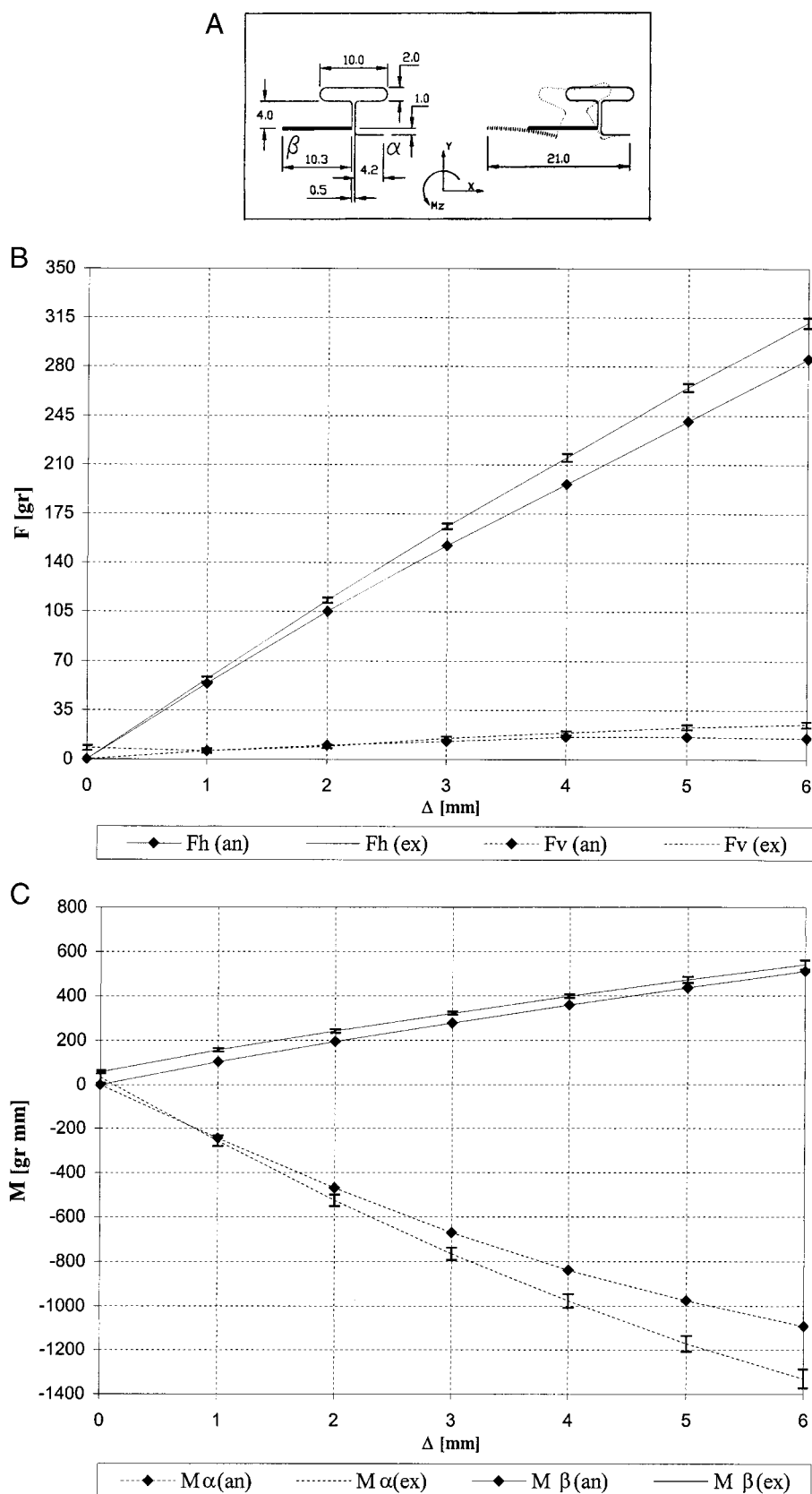


FIGURE 1. Test 1. (A) Continuous heavy line: 0.017" \times 0.025". Continuous light line: Φ 0.018". Dotted lines: after horizontal activation. Scale = 1/1. (B) Comparison between experimental (Ex) and analytical (An) results for forces. (C) Comparison between experimental (Ex) and analytical (An) results for moments.

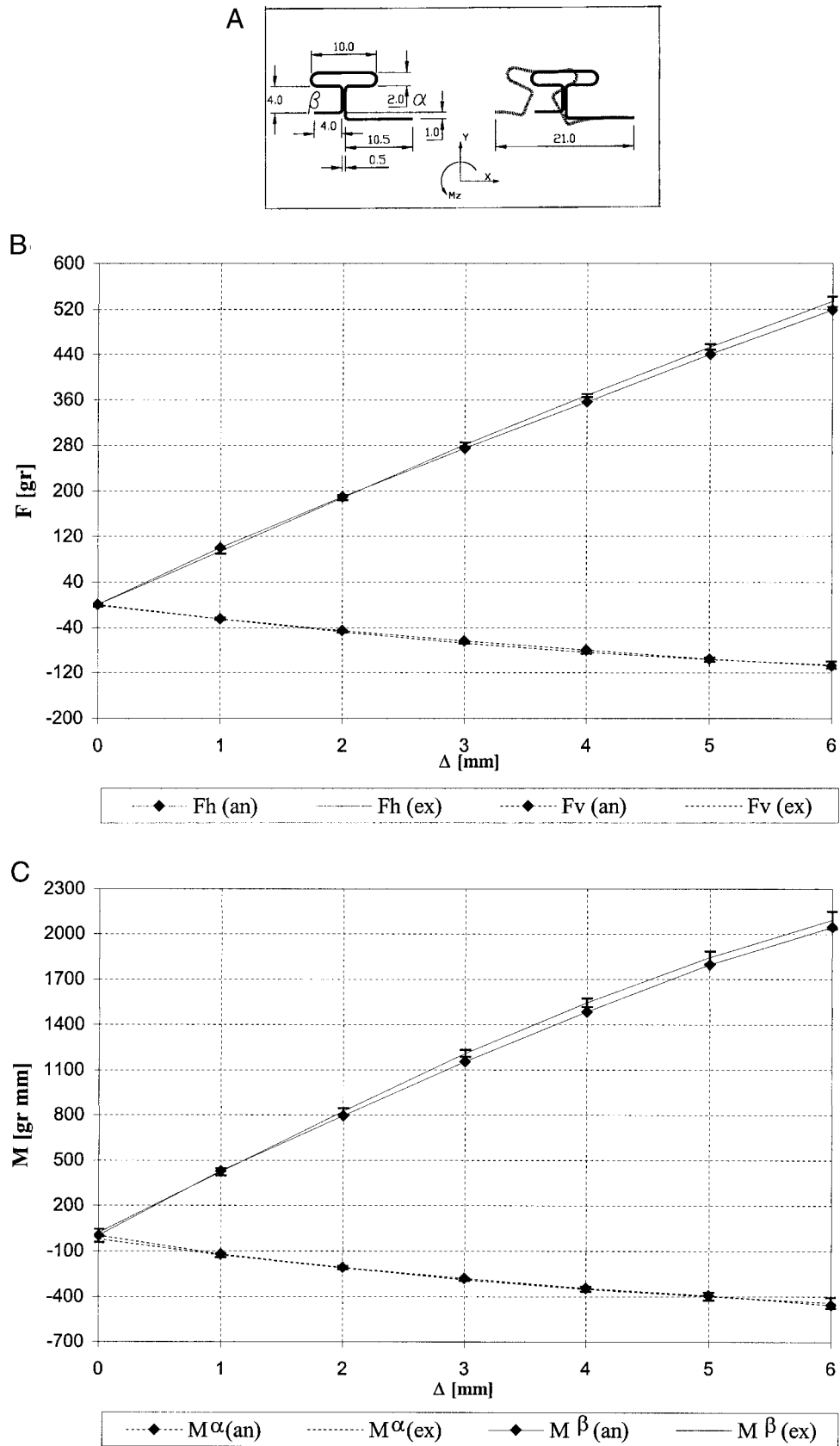


FIGURE 2. Test 2. (A) Dotted line: after horizontal activation. Scale = 1/1. (B) Comparison between experimental (Ex) and analytical (An) results for forces. (C) Comparison between experimental (Ex) and analytical (An) results for moments.

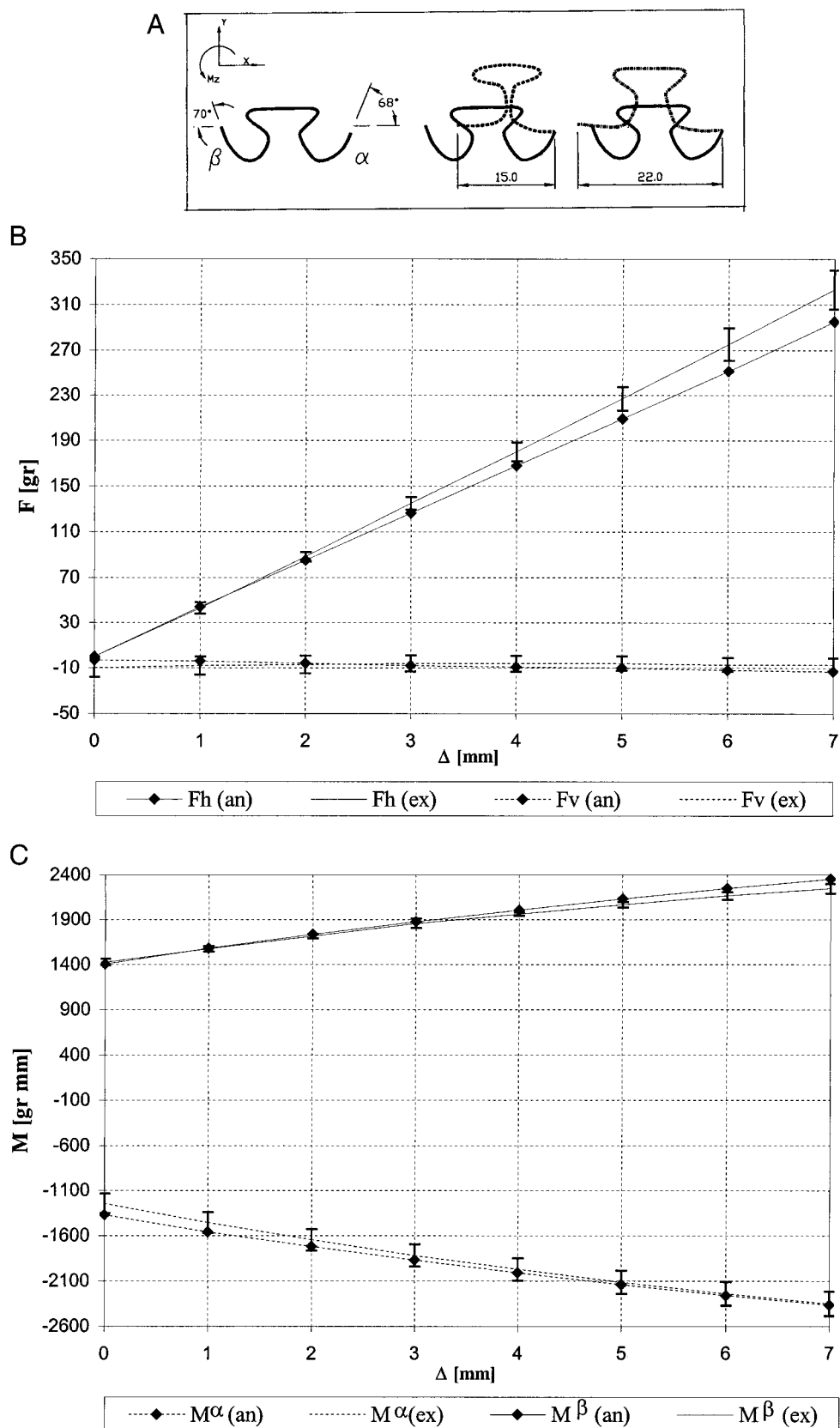


FIGURE 3. Test 3. (A) Dashed line: solid line after neutral activation; dash-dotted line: solid line after neutral and horizontal activations. Scale = 1/1. (B) Comparison between experimental (Ex) and analytical (An) results for forces. (C) Comparison between experimental (Ex) and analytical (An) results for moments.

lem of reliability of the software was solved, the true practical problem of analytically determining the preactivation shape of the spring in a specific clinical case remained.

In order to calculate at chairside the behavior of orthodontic springs in the segmented arch technique, a fourth series of studies was done, using a numerical approach based on a nonlinear finite element formulation with 2 nonlinear capabilities as large deflections and nonlinear elasticity.²⁰ Some verifications were done to test the precision of this approach. Of particular interest are the simulation of an experimentally determined T-loop spring and the solution of a benchmark exercise performed through a powerful commercial package. The approximations were within 19% and 7%, respectively. The nonlinear finite element formulation was combined with an algorithm capable of automatically computing the preactivation shape of the specialized springs.

Moreover, this software can be used on a personal computer, can perform computations in a short time, and does not require a highly trained user. The software is not commercially available at this time, but it is used in clinical practice by one of the authors (D. Mazza). An example of the clinical application of the analytical method at chairside has been shown.

Verification tests

Four verification tests were performed to further assess the reliability of the dedicated software. In each of these tests, a numerical simulation was carried out of a determined experimental condition performed by other researchers,^{1,8} after which a comparison was made between experimental and numerical results. The general scheme of the experimental conditions is presented here to better explain the simulations and their clinical purposes.

Four TMA T-loop springs relative to 4 different IBDs were prepared in the laboratory⁸ for each of the 3 basic TMA T-loop springs, for a total of 12 T-loop springs without preactivation bends.

A spring with preactivation bends was also developed for each 1 of the 12 springs, for a total of 12 T-loop springs with preactivation bends.

Each of the 12 T-loop springs without preactivation bends was mounted in 2 chucks of the spring tester and allowed to reach the *neutral position* (Appendix 1, B and C, solid line). The neutral position of a spring is defined as the geometry (of the spring) when no horizontal (mesiodistal) force is produced; it is measured as the distance between the 2 vertical legs of the spring.

Each of the 12 T-loop springs with preactivation bends (Appendix 1, D, solid line) was loaded in order to be mounted in the chucks of the spring tester and allowed to reach the neutral position (Appendix 1, E, dashed line), a procedure called *neutral activation*. In this position, only moments were acting on the springs; they were called *neu-*

tral activation moments to indicate that no horizontal forces were present.

From the neutral position, one end of each spring was pulled along the x-axis through the moveable carriage, a procedure called *horizontal activation* (Appendix 1, C, dotted line). The horizontal activation, Δ , was measured with respect to the neutral position of the spring.

Horizontal activation of the 24 springs was produced continuously, and changes of the force systems at each end were recorded in 0.5 mm increments. The force system is intended as measured at the α end of the wire.

In the laboratory, the instantaneous IBD along the x-axis was measured by chuck separation with the spring in a neutral position plus the horizontal activation.

Three springs for each experimental run were selected at random and each spring was run 3 times each. The mean and standard deviations for the α moment, β moment, horizontal force, and vertical force were calculated. The accuracy of the spring tester was approximately ± 4 g for the forces and ± 25 g mm for the moments.

The verified tests are now described.

Test 1 refers to a composite $0.017'' \times 0.025'' \times 0.18''$ TMA T-loop spring without preactivation bends (Figure 1A). In the laboratory, this spring which was 15 mm long in a neutral position was activated horizontally up to 6 mm. The geometrical data of this real spring⁸ were used for the simulation (Figure 1A, solid lines, heavy and light). Then the horizontal activation of the real spring was simulated, imposing at the β end of the analytical spring a horizontal displacement by 1 mm increments up to 6 mm. All other movements were prohibited at both ends. A horizontal activation of 6mm is shown (Figure 1A, dotted lines).

Test 2 refers to a $0.017'' \times 0.025''$ posterior protraction TMA T-loop spring without preactivation bends (Figure 2A; Appendix 1, B). In the laboratory, this spring, which was 15 mm long in a neutral position (Appendix 1, C, solid line), was activated horizontally up to 6 mm (Δ in Appendix 1, C, dotted line). The geometrical data⁸ of the real spring were used for the simulation (Figure 2A, solid line). Using the same boundary conditions as in test 1, the horizontal activation up to 6 mm was simulated (Figure 2A, dotted line).

Test 3 refers to a $0.017'' \times 0.025''$ attraction TMA T-loop spring with preactivation bends⁸ (Figure 3A, solid line, Appendix 1, D). In the laboratory, the spring was loaded so that it could be mounted in the chucks and allowed to reach the neutral position (Appendix 1, E). In this condition, the spring was subjected to neutral activation moments and was 15 mm long. Then it was subjected to a horizontal activation up to 7 mm. In order to simulate the neutral position of the real T-loop tested in the laboratory, the published template of the preactivation shape⁸ was entered into a digitizer (Figure 3A, solid line). Then -68° rotation at the α end and $+70^\circ$ rotation at the β end were imposed on the cross-section of the template, causing both ends of the

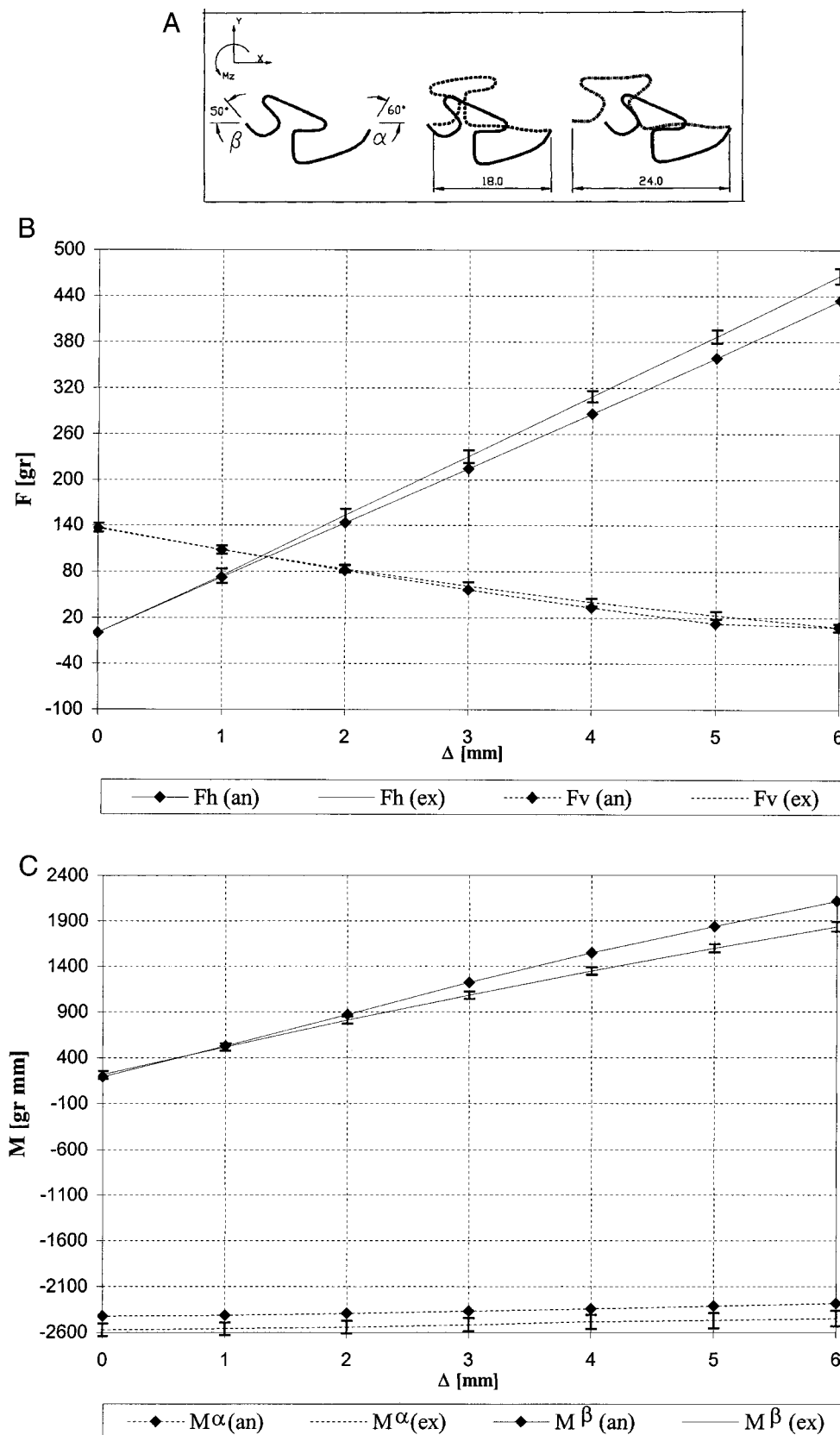


FIGURE 4. Test 4. (A) Dashed line: solid line after neutral activation; dash-dotted line: solid line after neutral and horizontal activations. Scale = 1/1. (B) Comparison between experimental (Ex) and analytical (An) results for forces. (C) Comparison between experimental (Ex) and analytical (An) results for moments.

TABLE 1. Test 1: Experimental (Ex) and Analytical (An) Results*

Δ , mm	Fh, g			Fv, g			M α , g mm			M β , g mm		
	An	Ex (Mean)	Ex (SD)	An	Ex (Mean)	Ex (SD)	An	Ex (Mean)	Ex (SD)	An	Ex (Mean)	Ex (SD)
0	0	0	0.0	0	8	1.7	0	33	25.6	0	57	7.7
1	54	57	1.8	6	6	1.5	-245	-258	24.0	102	156	7.8
2	105	113	1.9	10	9	1.2	-469	-526	25.9	193	241	8.0
3	152	166	2.0	13	15	1.2	-671	-766	28.6	278	322	7.0
4	196	215	2.8	16	19	1.5	-839	-977	30.6	359	399	8.3
5	241	265	2.9	16	23	1.8	-976	-1171	35.3	436	472	13.2
6	285	311	3.8	15	25	2.1	-1091	-1330	43.1	510	539	20.9

* Δ indicates horizontal displacement; Fh, horizontal force; Fv, vertical force; M α , alpha moment; M β , beta moment; and SD, standard deviation. Experimental data from Sachdeva.⁸

TABLE 2. Test 1: Percentage Differences Between Experimental (Ex) and Analytical (An) Results*

Δ , mm	Fh, %	Fv, %	M α , %	M β , %
1	-5.3	0.0	-5.0	-34.6
2	-7.1	11.1	-10.8	-19.9
3	-8.4	-13.3	-12.4	-13.7
4	-8.8	-15.8	-14.1	-10.0
5	-9.1	-30.4	-16.7	-7.6
6	-8.4	-40.0	-18.0	-5.4

* Δ indicates horizontal displacement; Fh, horizontal force; Fv, vertical force; M α , alpha moment; and M β , beta moment.

TABLE 4. Test 2: Percentage Differences Between Experimental (Ex) and Analytical (An) Results*

Δ , mm	Fh, %	Fv, %	M α , %	M β , %
1	6.4	0.0	-6.2	1.4
2	0.5	-4.2	-1.9	-3.5
3	-2.5	-5.9	-3.1	-4.5
4	-3.3	-4.8	-2.0	-3.9
5	-2.9	-1.0	-1.5	-2.6
6	-2.8	1.9	3.6	-2.2

* Δ indicates horizontal displacement; Fh, horizontal force; Fv, vertical force; M α , alpha moment; and M β , beta moment.

spring to lie horizontally. As in the laboratory, the only displacement allowed was the horizontal one at the β end, and the length reached by the analytical spring in neutral position was 15 mm (Figure 3A, dashed line) as in the laboratory.

Furthermore, the same template was subjected to neutral and horizontal activations using the same boundary conditions used to simulate the neutral position, except by imposing a horizontal displacement Δ up to 7 mm by 1 mm increments at the β end. The template now assumes a new shape (Figure 3A, dash-dotted line).

Test 4 refers to a 0.017" \times 0.025" posterior protraction TMA T-loop spring with preactivation bends¹ (Figure 4A). In the laboratory, the spring with preactivation bends was 18 mm long after having been mounted in the chucks and

after having reached the neutral position. The spring was then horizontally activated up to 6 mm. In order to simulate the neutral position of the real T-loop tested in the laboratory, the published template¹ of the preactivation shape was entered into a digitizer (Figure 4A, solid line). The same boundary conditions were used as in test 3 (the imposed rotations having been -60° at the α end and $+50^\circ$ at the β end). As in the laboratory, the analytical spring in its neutral position was 18 mm long (Figure 4A, dashed line).

Furthermore, the same template was subjected to neutral and horizontal activations using the same boundary conditions as in test 3, except the horizontal displacement Δ was up to 6 mm. The template now assumes a new shape (Figure 4A, dash-dotted line).

All the data of the problem have been presented at each

TABLE 3. Test 2: Experimental (Ex) and Analytical (An) Results*

Δ , mm	Fh, g			Fv, g			M α , g mm			M β , g mm		
	An	Ex (Mean)	Ex (SD)	An	Ex (Mean)	Ex (SD)	An	Ex (Mean)	Ex (SD)	An	Ex (Mean)	Ex (SD)
0	0	0	0.0	0	-1	2.5	0	-24	20.0	0	20	22.0
1	100	94	4.2	-25	-25	1.8	-121	-129	13.2	427	421	22.9
2	189	188	4.7	-46	-48	1.0	-207	-211	10.6	796	825	22.3
3	274	281	3.7	-64	-68	0.5	-279	-288	8.9	1156	1210	23.1
4	356	368	2.8	-80	-84	2.0	-345	-352	16.4	1484	1545	28.4
5	440	453	4.6	-96	-97	3.9	-394	-400	25.7	1796	1844	41.7
6	518	533	9.1	-108	-106	6.2	-457	-441	35.9	2046	2093	58.3

* Δ indicates horizontal displacement; Fh, horizontal force; Fv, vertical force; M α , alpha moment; M β , beta moment; and SD, standard deviation. Experimental data from Sachdeva.⁸

TABLE 5. Test 3: Experimental (Ex) and Analytical (An) Results*

Δ , mm	Fh, g			Fv, g			M α , g mm			M β , g mm		
	An	Ex (Mean)	Ex (SD)	An	Ex (Mean)	Ex (SD)	An	Ex (Mean)	Ex (SD)	An	Ex (Mean)	Ex (SD)
0	0	0	0.0	-3	-10	7.8	-1369	-1245	108.3	1407	1427	38.0
1	44	43	5.1	-4	-8	7.9	-1560	-1456	114.8	1581	1576	31.1
2	85	88	4.2	-6	-7	7.7	-1723	-1648	118.5	1734	1715	25.4
3	126	135	5.6	-8	-6	7.2	-1871	-1819	122.6	1875	1858	52.7
4	168	180	8.3	-9	-6	6.9	-2009	-1973	123.6	2007	1960	21.5
5	209	227	10.2	-10	-6	6.4	-2138	-2115	126.9	2131	2067	30.2
6	251	275	14.3	-12	-7	6.2	-2259	-2240	128.1	2247	2163	40.8
7	295	323	17.2	-13	-7	5.7	-2367	-2352	135.0	2351	2245	52.5

* Δ indicates horizontal displacement; Fh, horizontal force; Fv, vertical force; M α , alpha moment; M β , beta moment; and SD, standard deviation. Experimental data from Sachdeva.⁸

TABLE 6. Test 3: Percentage Differences Between Experimental (Ex) and Analytical (An) Results*

Δ , mm	Fh, %	Fv, %	M α , %	M β , %
1	2.3	-50.0	7.1	0.3
2	-3.4	-14.3	4.6	1.1
3	-6.7	33.3	2.9	0.9
4	-6.7	50.0	1.8	2.4
5	-7.9	66.7	1.1	3.1
6	-8.7	71.4	0.8	3.9
7	-8.7	85.7	0.6	4.7

* Δ indicates horizontal displacement; Fh, horizontal force; Fv, vertical force; M α , alpha moment; and M β , beta moment.

simulation, with the exception of the previously published TMA's modulus of elasticity.²⁰

Experimental and analytical results and their comparisons

The experimental^{1,8} and analytical results relative to tests 1, 2, 3, and 4 are shown in Tables 1, 3, 5, and 7, respectively.

The percentage differences between experimental and analytical results for the 4 tests are shown in Tables 2, 4, 6, and 8.

The data of Tables 1, 3, 5, and 7 are plotted in Figures

1B, 2B, 3B, and 4B, respectively, for forces, and in Figures 1C, 2C, 3C, and 4C for moments.

Two types of comparisons were made. First, comparisons were made between experimental and theoretical force systems in the 4 tests. Only horizontal forces and moments were taken into consideration because the percentage difference relative to small vertical forces is insignificant. Other authors dealing with the same problem followed the same criterion.¹⁷

The analytical approximation for the horizontal force in all 4 tests and for all the activations was within 10%. The analytical approximation for both moments in tests 2 and 3 was less than 10%, notwithstanding the nonlinearity of experimental data, the great deflections, and a slight asymmetry. A test similar to test 3 was performed by other authors with the same approximation.¹⁷ The importance of this test in evaluating the capability of nonlinear analysis by the software has been recognized by these authors as well, given the presence of great deflections coupled with asymmetry. The analytical approximation for both moments in tests 1 and 4 was within 18%. In test 1, this discrepancy can be attributed to the presence of 2 different cross-sections of the wire and 2 electrical welding spots. In test 4, the software had to deal with the presence of large deflections coupled with large asymmetries.

TABLE 7. Test 4: Experimental (Ex) and Analytical (An) Results*

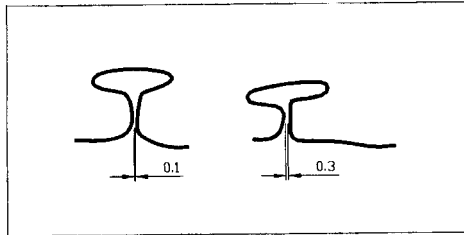
Δ , mm	Fh, g			Fv, g			M α , g mm			M β , g mm		
	An	Ex (Mean)	Ex (SD)	An	Ex (Mean)	Ex (SD)	An	Ex (Mean)	Ex (SD)	An	Ex (Mean)	Ex (SD)
0	0	0	0.0	136	137	5.8	-2427	-2574	69.0	190	215	42.2
1	72	74	9.4	108	108	5.4	-2415	-2562	66.1	528	516	38.5
2	143	153	8.7	81	83	5.1	-2395	-2543	69.0	873	810	40.6
3	214	230	8.3	56	61	5.4	-2371	-2519	72.2	1222	1080	39.1
4	286	309	7.6	33	40	5.0	-2343	-2487	76.8	1545	1346	39.2
5	359	387	8.6	12	23	5.1	-2314	-2472	80.8	1835	1595	45.8
6	434	466	9.9	7	7	5.1	-2284	-2449	86.0	2109	1832	53.6

* Δ indicates horizontal displacement; Fh, horizontal force; Fv, vertical force; M α , alpha moment; M β , beta moment; and SD, standard deviation. Experimental data from Burstone.¹

TABLE 8. Test 4: Percentage Differences Between Experimental (Ex) and Analytical (An) Results*

Δ , mm	Fh, %	Fv, %	$M\alpha$, %	$M\beta$, %
1	-2.7	0.0	-5.7	2.3
2	-6.5	-2.4	-5.8	7.8
3	-7.0	-8.2	-5.9	13.1
4	-7.4	-17.5	-5.8	14.8
5	-7.2	-47.8	-6.4	15.0
6	-6.9	0.0	-6.7	15.1

* Δ indicates horizontal displacement; Fh, horizontal force; Fv, vertical force; $M\alpha$, alpha moment; and $M\beta$, beta moment.

**FIGURE 5.** The analytical neutral position in tests 3 and 4. Scale = 1/1.

Second, comparisons were made between experimental and theoretical neutral activation shapes in test 3 and 4. In both tests, the comparison showed the following meaningful characteristics: (a) after the neutral activation, the analytical spring reached the same length (along the x-axis) as the real spring, and (b) after the neutral activation, the shortest distance between the vertical legs of the real T-loop (called the neutral position) was practically the same as between the 2 analytical vertical legs. In fact, the vertical legs were just touching in the laboratory^{1,8} and the smallest gap between the analytical vertical legs was 0.1 mm in test 3 and 0.3 mm in test 4 (Figure 5).

CONCLUSION

The approximations we obtained were within 18%. This precision was obtained for springs with a wide variety and combination of parameters, such as shape and size of the wire cross section, position of the T-loop along the IBD, absence or presence of the preactivation bends and length of the IBD.

It is important to simulate precalibrated springs in the laboratory for clinical use if computed springs are to be used clinically (Figure 6). The real template simulated in test 3 has been published¹ in order to be clinically used in the "en masse" horizontal bodily movement of 4 (or 6) anterior teeth for a clinical IBD of 22 mm. The real template simulated in test 4 has been published¹ in order to obtain the protraction of the posterior teeth with a clinical IBD of 24mm. The precision of the simulations in tests 3 and 5 was within 10% and 18%, respectively.

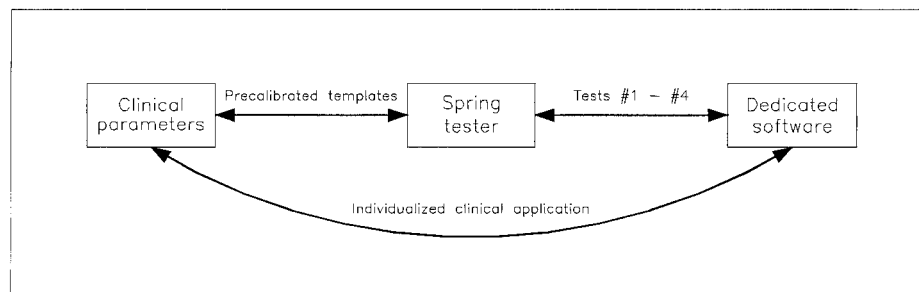
The approximations obtained in the 4 tests seem to be acceptable in order to use calculated specialized springs for individual clinical application.

In individualized clinical applications, the software requires automatic determination of the preactivation shape of the specialized springs. The basic algorithm necessary for this determination has been described previously.²⁰ A more complex algorithm is needed in the case of space closure, a topic to be discussed in a separate paper.

A computational efficiency for individualized clinical applications is also needed. As an example, the neutral activation and horizontal activation of up to 6 mm in test 4 was performed in 3.5 seconds using a Pentium 200 microprocessor.

REFERENCES

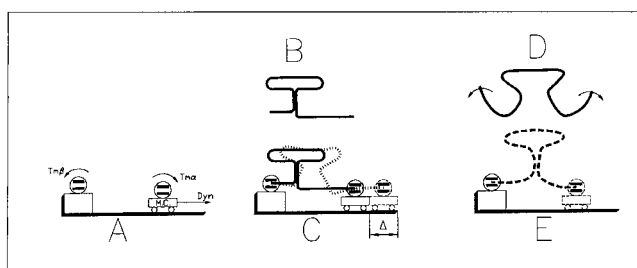
- Burstone CJ. *Modern Edgewise Mechanics Segmented Arch Technique*. Farmington, Conn: University of Connecticut; 1989.
- Burstone CJ. Deep overbite correction by intrusion. *Am J Orthod*. 1977;72:1-22.
- Romeo DA, Burstone CJ. Tip-back mechanics. *Am J Orthod*. 1977;72:414-421.
- Solonche DJ, Burstone CJ, Vanderby R. A device for determining the mechanical behavior of orthodontic appliances. *IEEE*. 1977; 24:538-539.
- Burstone CJ, Van Steenberg E, Hanley KJ. *Modern Edgewise Mechanics and the Segmented Arch Technique*. Farmington, Conn: University of Connecticut; 1995.
- Burstone CJ, Koenig HA. Optimizing anterior and canine retraction. *Am J Orthod*. 1976;70:1-20.
- Burstone CJ. The segmented arch approach to space closure. *Am J Orthod*. 1982;82:361-378.
- Sachdeva RC. *A Study of Force Systems Produced by TMA T-loop Retraction Spring* [thesis]. Farmington, Conn: University of Connecticut; 1985.
- Waters NE. The mechanics of plain and looped arches. *Br J Orthod*. 1975;3:161-167.

**FIGURE 6.** Interactions between experimental engineering, analytical engineering and clinical parameters.

10. Yang TY. Matrix displacement solution of elastic problems of beams and frames. *Int J Solids Structures*. 1973;9:829-842.
11. Yang TY, Baldwin JJ. Analysis of space closing springs in orthodontics. *J Biomech*. 1974;7:21-28.
12. Koenig HA, Burstone CJ. Analysis of generalized curved beams for orthodontic appliances. *J Biomech*. 1974;7:429-435.
13. DeFranco JC, Koenig HA, Burstone CJ. Three-dimensional large displacement analysis of orthodontic appliances. *J Biomech*. 1976;9:793-801.
14. Koenig HA, Vanderby R, Solonche DJ, Burstone CJ. Force systems from orthodontic appliances: an analytical and experimental comparison. *J Biomech Eng*. 1980;102:294-300.
15. Burstone CJ, Koenig HA. Precision adjustment of the transpalatal lingual arch: computer arch form predetermination. *Am J Orthod*. 1981;79:115-133.
16. Faulkner MG, Fuchsüber P, Haberstock D, Mioduchowski A. A parametric study of the force moment systems produced by T-loop retraction systems. *J Biomech*. 1989;22:637-47.
17. Lipsett AW, Faulkner MG, El-Rayes K. Large deformation analysis of orthodontic springs. *J Biomech Eng*. 1990;112:29-37.
18. Faulkner MG, Stredulinsky DC. Nonlinear bending of inextensible thin rods under distributed and concentrated loads. *Trans Can Soc Mech Eng*. 1977;4:77-82.
19. Raboud D, Faulkner MG, Lipsett AW. A segmental approach for large three-dimensional rod deformations. *Int J Solids Structures*. 1996;33:1137-56.
20. Mazza D, Mazza M. Specialized spring design in segmented edgewise orthodontics. *Am J Orthod Dentofacial Orthop*. 1997; 112:684-693.

APPENDIX 1.

(A) Idealized spring tester; $TM\beta$ and $TM\alpha$ indicate chucks with torque meters; Dyn, force meter; and M.C., moveable carriage (along with x-axis). (B) Eccentric T-loop spring without preactivation bends. (C) Same spring secured into chucks. Dotted line indicates that from the neutral position, the spring has been subjected to the horizontal activation Δ . (D) Centered T-loop spring with preactivation bends. (E) Same spring, loaded with moments and secured into chucks. The carriage moves until the spring reaches the neutral position (no horizontal forces present); now only moments (neutral moments or residual moments) are acting on the spring. From the neutral position, the spring will be subjected to the horizontal activation Δ as well (not shown).



APPENDIX 2.

Entered values in the computer in the case of test 1.

```

Automatic generation of a TMA T-loop spring without preactivation bends
Dimensions [mm]  1) Inter-bracket distance ..... = 15.0000
                  2) Alpha end Y coordinate(*) ..... = -1.0000
                  3) Spring's total height(*) ..... = 6.0000
                  4) Distance(*) to the center of the T ..... = 10.5000
Wire section["]  5) B ..... = 0.0243
                  6) H ..... = 0.0168
                  7) R ..... = 0.0180
                  8) Beta horizontal displacement [mm] .. = 6.0000
                  9) Step [mm] ..... = 0.5000

Press:
  any number from 1 to 9 to modify parameters
  0 to calculate the spring .....
  -1 to quit .....

(*) = Referred to beta end
    
```